

# Quantum Information of Photon Pairs at Lepton Colliders

Kun Cheng,<sup>1,\*</sup> Tao Han,<sup>1,†</sup> Guanghui Li,<sup>2,3,‡</sup> and Bin Yan<sup>2,4,§</sup>

<sup>1</sup>*PITT PACC, Department of Physics and Astronomy,*

*University of Pittsburgh, 3941 O'Hara St., Pittsburgh, PA 15260, USA*

<sup>2</sup>*Institute of High Energy Physics, Chinese Academy of Sciences, Beijing 100049, China*

<sup>3</sup>*School of Physical Sciences, University of Chinese Academy of Sciences, Beijing 100049, China*

<sup>4</sup>*Center for High Energy Physics, Peking University, Beijing 100871, China*

Photon pairs have provided an ideal laboratory for exploring entanglement and Bell inequality violation in low-energy experiments. Extending such studies to high-energy colliders is of great interest but has yet to be explored. Exploiting the photon conversion process for nearly on-shell photons, we formulate a factorization framework and an effective two-qubit description, which enable access to quantum information encoded in photon pairs. Using the existing Belle data set, we estimate that a  $7.4\sigma$  violation of the Bell inequality could be achieved. The same framework can also probe quantum discord and nonstabilizerness, which could be measured with precisions of 5.6% and 1.6%, respectively. All the reconstructed results from photon conversion in the two-qubit framework are found to be consistent with the kinematic approach of real photons, and the formalism can apply to other spin-1 systems in an appropriate two-qubit limit.

*Introduction* — Photons have provided an ideal platform for studying the most characteristic quantum phenomena, enabling early measurements of spin correlations between two particles [1], pioneering tests of Bell inequalities [2–4], and establishing the violation of Bell inequalities and ushering quantum information science [5].

Recent progress in studying quantum correlation in high-energy collisions has opened a new avenue in exploring quantum information science with a plethora of data in high-energy experiments [6–69], signified by the observation of spin entanglement of top quark pair [70, 71] and  $H \rightarrow ZZ^* \rightarrow \ell^+\ell^-\ell^+\ell^-$  [41, 42] at the Large Hadron Collider (LHC). It is understood that, given the particle identification capabilities of the current detector technologies, high-energy experiments do not offer Alice-Bob's setting originally proposed by John Bell [72] to test realism or to generally exclude interpretation by local hidden variable theories [73–78]. Instead, the focus has been on understanding quantum information within the framework of quantum field theory and exploring new interactions beyond the Standard Model [79].

There are two complementary approaches to establishing the spin-entanglement with high-energy data. One is to rely on the production of a quantum state without requiring the subsequent decays, dubbed the “kinematic approach” [80]. This is the original method for extracting spins for light quarks [81] and gluons [82, 83]. Without the capability of a polarizer, the spin information of the photons and electrons observed in an electromagnetic calorimeter or a tracker would only be inferred from kinematic distributions. Another more informative approach is to follow the decays after the production of the quantum state, including  $t\bar{t}$  [6–17],  $\tau^+\tau^-$  [18–25], and vector bosons [26–42]. Along this approach, we consider a quantum ensemble of correlated photon pairs as a bi-qubit system and propose to obtain quantum information of photons by exploiting photon conversion into lepton pairs

$\gamma^* \rightarrow \ell^+\ell^-$ . This spin correlation has proven to be important in determining fundamental quantum numbers such as the CP property of  $\pi^0$  [84, 85].

For a spin-1 vector boson, the massive particle (or an off-shell photon) has three polarization states, thus effectively forming a qutrit. However, in certain circumstances, a vector boson can be simplified as a qubit while preserving all quantum information. We demonstrate this by exploiting a nearly on-shell photon conversion, which can be factorized from the hard production dynamics, and the two physical polarization states form an effective qubit.

In this Letter, we develop a factorization and quantum tomography framework for photon conversion processes, which reconstructs the linear polarizations of the two-photon polarization density matrix of two qubits in the nearly on-shell limit. This thereby enables and significantly simplifies collider measurements of quantum information of photons. As an application, we study photon pair production in Belle [86] and find that a violation of the Clauser–Horne–Shimony–Holt (CHSH) inequality [87] could be established at the level of  $7.4\sigma$  using the existing data set, with the improved sensitivity expected in the Belle II experiment due to its larger data sample [88]. For configurations with negatively correlated photon helicities in the on-shell limit, the same framework can also be applied to other quantum information observables. In particular, quantum discord could be measured to a precision of 5.6%, while nonstabilizerness could be measured to 1.6%. We demonstrate the consistency between reconstructed results and the kinematic approach, which, for the first time, shows the validity of the qubit treatment of virtual photons from the quantum information aspect.

*Spin state for nearly on-shell photon pair* — We consider a correlated two-photon system produced in

$$e^+e^- \rightarrow \gamma^*\gamma^* \rightarrow \ell_1^+\ell_1^-\ell_2^+\ell_2^-, \quad (1)$$

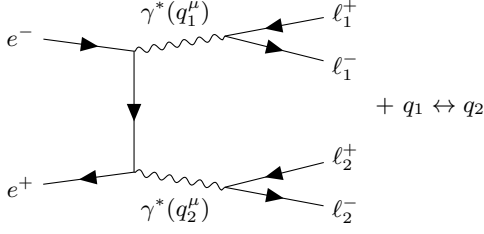


FIG. 1. Feynman diagrams for photon-pair production at a lepton collider followed by virtual-photon conversions into lepton pairs.

as shown in Fig. 1. The two virtual photons are produced and subsequently converted into lepton pairs. The invariant mass of each photon is given by  $q_i^2 = m_{\ell_i^+ \ell_i^-}^2$ , and we define the virtuality of the photon with respect to the scattering center-of-mass (c.m.) energy  $\sqrt{s}$  as  $\delta_i = \sqrt{q_i^2}/\sqrt{s}$ .

The propagator of a virtual photon with momentum  $q$  can be decomposed as

$$g^{\mu\nu} = \frac{q^\mu q^\nu}{q^2} - \sum_{\lambda=0,\pm 1} \epsilon_\lambda^\mu(q) \epsilon_{\lambda'}^{\nu*}(q). \quad (2)$$

Since the final-state lepton pair produced from each virtual photon carries identical masses, the  $q^\mu q^\nu/q^2$  term does not contribute to the amplitude due to current conservation. The squared amplitude can therefore be written in a factorized form,

$$|\mathcal{M}|^2 = \frac{1}{q_1^4 q_2^4} \sum_{\lambda=0,\pm 1} R_{\lambda_1 \lambda'_1, \lambda_2 \lambda'_2} \Gamma_{\lambda_1 \lambda'_1}^{(1)} \Gamma_{\lambda_2 \lambda'_2}^{(2)}. \quad (3)$$

Here,  $R_{\lambda_1 \lambda'_1, \lambda_2 \lambda'_2}$  is the unnormalized production spin density matrix of the virtual photon pair,

$$R_{\lambda_1 \lambda'_1, \lambda_2 \lambda'_2} = \sum_{\sigma \bar{\sigma}} \mathcal{M}(e_\sigma^- e_{\bar{\sigma}}^+ \rightarrow \gamma_{\lambda_1} \gamma_{\lambda_2}) \mathcal{M}(e_{\bar{\sigma}}^- e_\sigma^+ \rightarrow \gamma_{\lambda'_1} \gamma_{\lambda'_2})^*, \quad (4)$$

where  $\sigma$  and  $\bar{\sigma}$  are the helicities of the initial-state electron and positron, while  $\lambda_i$  and  $\lambda'_i$  denote the helicities of the virtual photons. The quantity  $\Gamma_{\lambda, \lambda'}^{(i)}$  is the ‘‘splitting density matrix’’ associated with the conversion of the  $i$ -th virtual photon into a lepton pair,

$$\Gamma_{\lambda \lambda'}^{(i)} = \sum_{s, \bar{s}} \left( \bar{\ell}_i \not{\epsilon}_\lambda(q_i) \ell_i \right) \left( \bar{\ell}_i \not{\epsilon}_{\lambda'}(q_i) \ell_i \right)^*, \quad (5)$$

where the helicities  $s$  and  $\bar{s}$  of the final-state lepton and antilepton are summed over.

The spin indices of the virtual photon in Eq. (3) sum over both transverse and longitudinal modes. The spin state of a virtual photon is therefore described by a qutrit state, as any massive spin-1 particle in general. However, when both photons are close to the mass shell

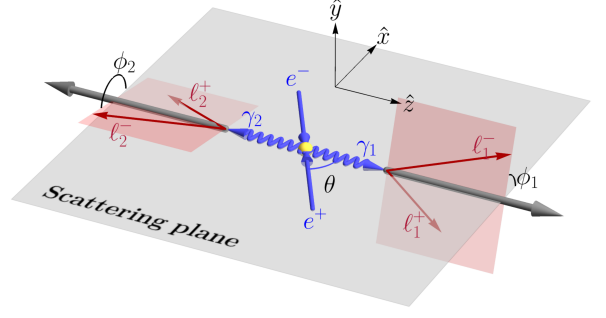


FIG. 2. Leading order kinematic configuration of photon pair production with virtual-photon conversions into lepton pairs in  $e^- e^+$  collisions.

( $\delta_i \rightarrow 0$ ), the longitudinal polarization vector becomes proportional to the photon momentum,

$$\epsilon_0^\mu(q_i) = \frac{q_i^\mu}{\sqrt{q_i^2}} + \mathcal{O}(\delta_i), \quad (6)$$

so that the longitudinal contributions to both the production density matrix  $R$  and the splitting density matrix  $\Gamma^{(i)}$  are suppressed. The scattering process can therefore be effectively described by the transverse components,

$$\frac{d\sigma}{d\Omega} \propto \sum_{\lambda=\pm 1} R_{\lambda_1 \lambda'_1, \lambda_2 \lambda'_2} \Gamma_{\lambda_1 \lambda'_1}^{(1)} \Gamma_{\lambda_2 \lambda'_2}^{(2)} + \mathcal{O}(\delta^2). \quad (7)$$

Consequently, up to  $\mathcal{O}(\delta^2)$  corrections, the spin state of the virtual photon pair in the process  $e^- e^+ \rightarrow \gamma^* \gamma^* (\rightarrow \ell_1^+ \ell_1^- \ell_2^+ \ell_2^-)$  can be effectively treated as a qubit pair. The corresponding normalized  $4 \times 4$  spin density matrix,  $\rho = R/\text{tr}(R)$ , can be parametrized as,

$$\rho = \frac{I_2 \otimes I_2 + B_i^{(1)} \sigma_i \otimes I_2 + B_i^{(2)} I_2 \otimes \sigma_i + C_{ij} \sigma_i \otimes \sigma_j}{4}, \quad (8)$$

where  $I_2$  is the 2-dimensional identity matrix and  $\sigma_i$  is the Pauli matrix. Here, we choose the same spin quantization axis for both photons, with the  $z$  direction defined along the momentum of  $\gamma_1$  (see Fig. 2), and the choice of  $\gamma_1$  is arbitrary due to identical particles. Then the eigenstates of  $\sigma_z$  correspond to the circular polarized photon with positive/negative helicity, while the eigenstates of  $\sigma_{x/y}$  correspond to linearly polarized states. The coefficients  $B_{x/y}^{(i)}$  and  $B_z^{(i)}$ , respectively, quantify the degree of linear and circular polarization of the  $i$ -th photon, while  $C_{ij}$  is the correlation matrix between the polarization of two photons.

Within this effective two-qubit description, the full quantum information is encoded in  $B^{(1)}, B^{(2)}$  and  $C_{ij}$ . One of the most characteristic quantum correlations is entanglement, which can be quantitatively described by the concurrence  $\mathcal{C}$ , defined as  $\mathcal{C} = \max\{0, \lambda_1 - \lambda_2 - \lambda_3 - \lambda_4\}$  where  $\lambda_i$  are the eigenvalues

in the descending order of the matrix  $\sqrt{\sqrt{\rho}\tilde{\rho}\sqrt{\rho}}$ , with  $\tilde{\rho} = (\sigma_2 \otimes \sigma_2)\rho^*(\sigma_2 \otimes \sigma_2)$  [89], and  $\mathcal{C} > 0$  implies an entangled state. A stronger condition than entanglement, the Bell inequality violation, can be measured with a simpler linear variable

$$\mathcal{B}_{\pm} = C_{xx} \pm C_{yy}. \quad (9)$$

The CHSH inequality states  $|\mathcal{B}_{\pm}| < \sqrt{2}$ , which can be violated by quantum mechanical predictions. The measured value of the Bell variable Eq. (9) also provides a lower bound of the entanglement between the two photons through the following relation [90],

$$\mathcal{C} \geq \sqrt{\frac{\mathcal{B}_{\pm}^2}{2} - 1}. \quad (10)$$

*Photon polarization from final state distribution* — With Eq. (7), the photon spin density matrix can be directly related to measurable final-state lepton distributions. As shown in Fig. 2, in the c.m. frame, photon conversion kinematics can be parametrized by the lepton azimuthal angle  $\phi$  and the light-cone momentum fraction

$$z = \frac{E_{\ell} + p_{\ell}^z}{E_{\gamma} + p_{\gamma}^z}. \quad (11)$$

In the collinear limit with small virtuality  $s \gg q^2$ ,  $z$  is approximately the energy fraction  $E_{\ell}/E_{\gamma}$ . In terms of these variables, the matrix  $\Gamma_{\lambda\lambda'}$  in Eq. (5) can be decomposed in the Pauli matrix basis as

$$\frac{1}{16q^2}\Gamma_{\lambda\lambda'} = D(z, q^2)\delta_{\lambda\lambda'} + H(z, q^2) \left[ \cos(2\phi)(\sigma_x)_{\lambda\lambda'} + \sin(2\phi)(\sigma_y)_{\lambda\lambda'} \right]. \quad (12)$$

Here, we define the functions  $D(z, q^2)$  and  $H(z, q^2)$  for  $\gamma^* \rightarrow \ell^+\ell^-$  in analogy to the fragmentation functions,

$$D(z, q^2) = \frac{1}{2} + \frac{m_{\ell}^2}{q^2} - z(1-z), \quad (13a)$$

$$H(z, q^2) = \frac{m_{\ell}^2}{q^2} - z(1-z), \quad (13b)$$

which, respectively, characterize the overall unpolarized conversion probability and the linear polarization dependence. Since the conversion process is invariant under charge conjugation, Eq. (12) is invariant under  $z \rightarrow (1-z)$  and  $\phi \rightarrow \phi + \pi$ . Consequently,  $\phi$  and  $z$  can be defined without specifying the charge of  $\ell^+$  or  $\ell^-$ .

To parametrize how sensitive the final state distribution depends on linear polarization, it is convenient to introduce the spin-analyzing power

$$\kappa_q^z = \frac{H(z, q^2)}{D(z, q^2)}. \quad (14)$$

When  $z = 1/2$ , the leptons have the largest transverse momentum to probe the azimuthal distribution and the

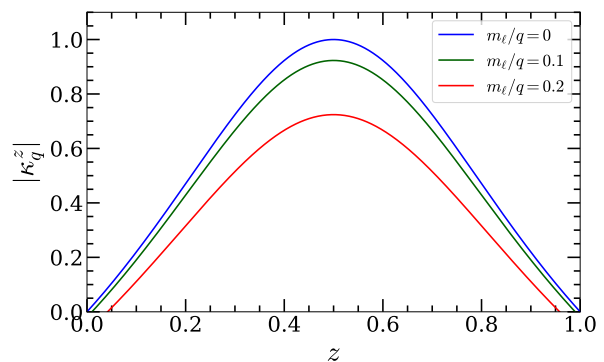


FIG. 3. Spin analyzing power as a function of splitting kinematics.

spin analyzing power reaches the maximum, as shown in Fig. 3. It decreases with  $m_{\ell}/q$  because the lepton pair tends to be co-moving without angle distributions with increasing masses.

The structure of Eq. (12) also reveals that no  $\sigma_z$  term appears in the splitting density matrix, which is a result of parity conservation of QED processes. Unlike quantum tomography utilizing parity-violating decays that can reconstruct the full spin density matrix [6], the degree of circular polarization of the photon cannot be accessed through the splitting process. Nevertheless, the full information on the linear polarization can be reconstructed and it is sufficient to construct observables sensitive to quantum correlations in two-photon systems.

With Eq. (12) and the parameterization of the photon pair spin density matrix, the differential distribution in Eq. (7) can be rewritten as

$$\frac{d\sigma}{d\Omega_1 d\Omega_2} \propto \frac{D(z_1, q_1^2)D(z_2, q_2^2)}{q_1^2 q_2^2} \sigma_{\text{hard}} \left[ 1 + \alpha_{q_1, q_2}^{z_1, z_2} \times (\mathcal{B}_- \cos 2(\phi_1 + \phi_2) + \mathcal{B}_+ \cos 2(\phi_1 - \phi_2)) \right]. \quad (15)$$

Here,  $d\Omega_i = dz_i dq_i^2 d\phi_i$  is the splitting phase space element,  $\sigma_{\text{hard}}$  is the cross section of the production of the real photon pair, and  $\alpha_{q_1, q_2}^{z_1, z_2} = \kappa_{q_1}^{z_1} \kappa_{q_2}^{z_2} / 2$  is the event-dependent spin analysis power.

The Bell variable can be directly reconstructed from the azimuthal distribution of the lepton pairs as

$$\mathcal{B}_{\mp} = 2 \frac{\langle \cos 2(\phi_1 \pm \phi_2) \rangle}{\langle \alpha_{q_1, q_2}^{z_1, z_2} \rangle}, \quad (16)$$

where  $\langle \mathcal{O} \rangle$  denotes the event average of the quantity  $\mathcal{O}$ . With  $N$  reconstructed events ( $N \gg 1$ ), we estimate the statistical uncertainty  $\delta\mathcal{B}$  and the significance as

$$\delta\mathcal{B} = \frac{\sqrt{2/N}}{\langle \alpha_{q_1, q_2}^{z_1, z_2} \rangle}, \quad \#\sigma = \frac{(\mathcal{B} - \sqrt{2})}{\delta\mathcal{B}}. \quad (17)$$

Alternatively, the inverse of the statistical significance  $1/\#\sigma$  serves as a measure of the precision of the measurement.

*Simulation and sensitivity* — We carry out a detailed study for the process  $e^+e^- \rightarrow \gamma^*\gamma^* \rightarrow \ell_1^+\ell_1^-\ell_2^+\ell_2^-$  in the Belle experiments [88] with  $\sqrt{s} = 10.58$  GeV. We perform a Monte-Carlo simulation using MADGRAPH [91]. Signal events are selected to contain exactly four charged leptons with zero net charge. To suppress background, all final-state leptons are required to satisfy  $E_\ell > 0.1$  GeV and  $|\cos\theta_\ell| < 0.9$  in the c.m. frame, which are within the acceptance of the Belle detector [88]. To enrich the event selection for near-on-shell photon pair conversion, the four-lepton event is selected by requiring  $m_{ee} < 0.5$  GeV for electron pairs and  $m_{\mu\mu} < 1$  GeV for muon pairs. These requirements suppress non-factorizable contributions and ensure the validity of the qubit approximation. To reconstruct the azimuthal asymmetry, we additionally require a minimal angular separation between the leptons of each reconstructed virtual photon. Taking advantage of the superb angular resolution,<sup>1</sup> we adopt a low threshold for the separation between the two leptons  $\Delta R = \sqrt{\Delta\phi^2 + \Delta\eta^2} > 0.001$ . After event selection, the signal cross sections for the  $2e^+2e^-$  ( $ee$ ),  $e^+e^-\mu^+\mu^-$  ( $e\mu$ ) and  $2\mu^+2\mu^-$  ( $\mu\mu$ ) channels are 0.15 pb, 0.076 pb and  $9.8 \times 10^{-3}$  pb, respectively. The residual background contributions remain at the level of approximately 7%, 4% and 1% for  $ee$ ,  $e\mu$  and  $\mu\mu$  channels, respectively. For the same-flavor  $ee$  and  $\mu\mu$  channels, possible combinatorial ambiguities in pairing leptons into virtual photon candidates are below 0.001% and 1% levels, respectively. The background and mis-pairing in total modify the reconstructed Bell variable by less than 5%, which do not qualitatively affect the sensitivity to Bell inequality violation and are therefore neglected in the following analysis.

Using the selected event sample, the Bell variable in Eq. (16) and its associated uncertainty are reconstructed from the simulated events using the analytical expression for the average of  $\alpha_{q_1, q_2}^{z_1, z_2}$ . Figure 4 shows the reconstructed values of  $\mathcal{B}_-$  in  $ee$  (blue),  $e\mu$  (red) and  $\mu\mu$  (green) channels for different selection cuts  $|\cos\theta| < c_{\text{cut}}$  of the photon angle  $\theta$ , with the statistical uncertainties scaled to an integrated luminosity of  $1 \text{ ab}^{-1}$ .

For real photon pair production, quantum tomography can also be achieved in the kinematic approach directly from the scattering angle  $\theta$  [80], with the Bell variable given by

$$\mathcal{B}_- = \frac{2 \sin^2 \theta}{1 + \cos^2 \theta}, \quad \mathcal{B}_+ = 0, \quad (18)$$

where  $\mathcal{B}_-$  reaches its maximal value 2 at  $\cos\theta = 0$ . For comparison, we also show the prediction in the kinematic

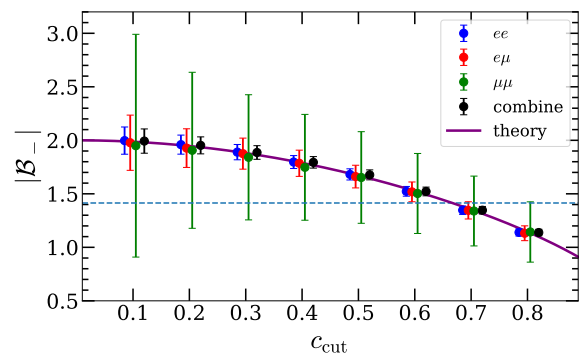


FIG. 4. Reconstructed Bell variable  $|\mathcal{B}_-|$  at Belle from photon conversion processes for different angular selections  $|\cos\theta| < c_{\text{cut}}$  and the requirement  $\Delta R > 0.001$ . The statistical uncertainties are estimated for an integrated luminosity of  $\mathcal{L} = 1 \text{ ab}^{-1}$ . The solid curve is from the prediction of the kinematic method in Eq. (18).

approach with the purple line in Fig. 4. We find the reconstructed central values agree with the prediction by the kinematic method, and the longitudinal mode contributions for low  $q^2$  are at  $\sim 1\%$  level or smaller, confirming the validity of the effective two-qubit description of the virtual photon pair.

As predicted by Eq. (18),  $\mathcal{B}_-$  is enhanced in the central scattering region. We consider a requirement  $|\cos\theta| < 0.3$ , which further reduces the background contributions by approximately 30%. With this selection, the significance of Bell inequality violation are  $6.6\sigma$ ,  $3.2\sigma$  and  $0.7\sigma$  for the  $ee$ ,  $e\mu$  and  $\mu\mu$  channels, respectively, at an integrated luminosity of  $1 \text{ ab}^{-1}$  comparable to the Belle data sample [93]. The  $\gamma^* \rightarrow e^+e^-$  channel is more sensitive than  $\gamma^* \rightarrow \mu^+\mu^-$  because of a larger spin analyzing power, as shown in Fig. 3. While detector effects may also reduce these significances, the much larger data set expected at the Belle II experiment would provide a robust environment for an experimental realization.

To further improve the statistical sensitivity, we combine the three channels using inverse-variance weighting,

$$\mathcal{B}_- = \frac{\sum_i \omega_i \mathcal{B}_-^i}{\sum_i \omega_i}, \quad (19)$$

where  $i = ee, e\mu, \mu\mu$  and the weights are defined as  $\omega_i = 1/(\delta\mathcal{B}_-^i)^2$ . The variance of the combined Bell variable is given by  $\text{Var}(\mathcal{B}_-) = 1/\sum_i \omega_i$ . The combined results are also shown as black points in Fig. 4. For the benchmark selection  $|\cos\theta| < 0.3$ , a  $7.4\sigma$  violation of the Bell inequality could be established at  $\mathcal{L} = 1 \text{ ab}^{-1}$ .

A similar analysis can also be performed at BEPC [94] at  $\sqrt{s} = 3.773$  GeV using the  $ee$  channel, since the two-qubit approximation breaks down for the muon final state. The same event selection as in the Belle analysis is adopted, except for a tighter requirement  $m_{ee} < 0.2$  GeV to further suppress backgrounds. Using the currently ac-

<sup>1</sup> The angle resolution of electron tracks at Belle and BaBar detectors can reach sub mrad level [86, 92].

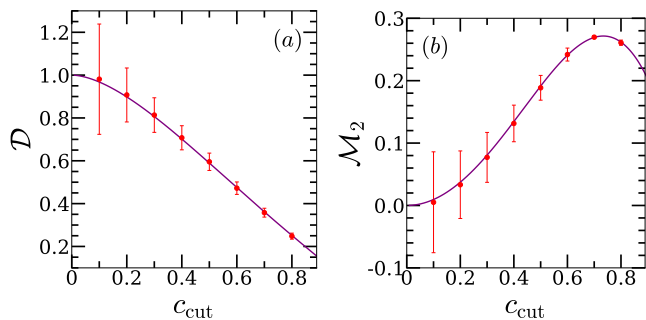


FIG. 5. Reconstructed quantum discord  $\mathcal{D}$  (a) and magic  $\mathcal{M}_2$  (b), in comparison with prediction from the kinematic approach of real photon pair production.

cumulated luminosity of  $20 \text{ fb}^{-1}$  [94], the expected significance reaches  $2.4\sigma$ . The sensitivity can be further improved with future luminosity upgrades, reaching the  $5\sigma$  level at  $\mathcal{L} = 88 \text{ fb}^{-1}$ .

*Other quantum information variables*— Although the photon conversion process does not directly provide access to the  $z$  components in the spin density matrix, the spin of two photons is guaranteed to be 100% negatively correlated along the  $z$  axis ( $C_{zz} = 1$ ) for on-shell photon states, and the spin correlation matrix is diagonal in the helicity basis. This structure allows any quantum information observable to be investigated with  $C_{xx/yy}$  reconstructed from Eq. (16). Here, we consider quantum discord and quantum magic as representative examples, while other observables can be evaluated in a similar way.

Quantum discord characterizes non-classical correlations more basic than entanglement. Quantum discord is defined as the difference between two classically identical expressions for mutual information [95], thus quantifying the non-classical correlation. For a two-qubit system, the discord reads [96]

$$\mathcal{D} \equiv S(\rho_B) - S(\rho_{AB}) + \min_{\{\Pi_k\}} p_k S(\rho_{A|k}), \quad (20)$$

where  $S(\rho) = -\text{Tr}(\rho \log_2 \rho)$  is the von Neumann entropy,  $\rho_{A/B} = \text{tr}_{B/A}(\rho_{AB})$  is the reduced density matrix for the first/second qubit, and  $\rho_{A|k}$  represents the post-measurement quantum states for the qubit  $\mathcal{A}$  given a projective measurement  $\Pi_k$  on the qubit  $\mathcal{B}$  with outcomes  $k$  and projection probability  $p_k$ . The quantum discord can be calculated analytically when the spin correlation matrix is diagonal [10, 16, 17, 97, 98]. The results for different angular cuts, combining the  $ee$ ,  $e\mu$ , and  $\mu\mu$  channels at an integrated luminosity of  $1 \text{ ab}^{-1}$  are shown in Fig. 5(a). A nonzero discord,  $0 < \mathcal{D} \leq 1$ , could be measured to a precision of 5.6% for  $c_{\text{cut}} = 0.8$ . We see again the consistency between the reconstructed results from the photon conversion and the solid line from the kinematic method.

Quantum magic describes the potential computational advantage of quantum states over classical states, and

can also provide a complementary description of the state configuration. Any stabilizer state can be effectively simulated on a classical computer and has zero magic, whereas quantum states with higher magic provide a greater computational advantage over classical systems. Quantum magic can be described by second stabilizer Rényi entropy  $\mathcal{M}_2$ , which is evaluated as [99–101]

$$\mathcal{M}_2 = -\log_2 \left( \frac{1 + \sum_i (B_i^{(1)})^4 + \sum_j (B_j^{(2)})^4 + \sum_{i,j} C_{ij}^4}{1 + \sum_i (B_i^{(1)})^2 + \sum_j (B_j^{(2)})^2 + \sum_{i,j} C_{ij}^2} \right). \quad (21)$$

As shown in Fig. 5(b), combining the  $ee$ ,  $e\mu$ , and  $\mu\mu$  channels at the same integrated luminosity, the quantum magic decreases with a smaller angular cut of  $|\cos\theta|$ , indicating that the state approaches a stabilizer Bell state in the central scattering region. The non-stabilizer nature could be measured to a precision of 1.6% for  $c_{\text{cut}} = 0.8$ . Again, the consistency between the solid line from the kinematic method and the reconstructed results shows the validity of the two-qubit framework.

*Conclusion*— We proposed a framework to probe quantum correlations of energetic photon pairs via their conversion into dilepton pairs in the small-virtuality regime. In this limit, the conversion process factorizes from the hard production dynamics, enabling the photon polarization state to be treated as a qubit state and inferred from final-state angular correlations. We demonstrated the feasibility of this approach using the existing Belle data sample. Backgrounds from nonfactorizable effects are found to be negligible after event selections, while the effective two-qubit description remains valid at the percent level. The  $ee$  splitting channel provides the most sensitive probe of quantum information due to its larger event yield and stronger spin-analyzing power. Combining the  $ee$ ,  $e\mu$ , and  $\mu\mu$  channels, a  $7.4\sigma$  observation of Bell inequality violation could be achieved at  $\mathcal{L} = 1 \text{ ab}^{-1}$ , while a positive quantum discord could be observed with a precision of 5.6%. Quantum magic analysis indicates that the state approaches a stabilizer Bell state in the central region, and the departure from the stabilizer regime could be measured to a precision of 1.6%. We found full consistency between the kinematic method and the reconstructed results from the photon conversion in the qubit approximation for spin-1 virtual photons. Our results establish photon conversion as a practical handle for accessing quantum properties of photons at colliders and identify photon pairs as a promising system for studying quantum entanglement in high-energy physics. The framework could also be extended to processes such as  $h \rightarrow \gamma\gamma$  at the LHC as well as the other spin-1 states in an appropriate qubit limit.

We thank C. Z. Yuan and M. Q. Ruan for helpful discussions. KC and TH were supported in part by the US Department of Energy under grant N. DE-SC0007914, and in part by Pitt PACC. GL and BY were partly sup-

ported by the National Natural Science Foundation of China under Grant No. 12422506, and CAS under Grant No. E429A6M1. The authors gratefully acknowledge the valuable discussions and insights provided by the members of the Collaboration on Precision Tests and New Physics (CPTNP).

---

\* kun.cheng@pitt.edu

† than@pitt.edu

‡ ghli@ihep.ac.cn

§ yanbin@ihep.ac.cn (corresponding author)

- [1] C. S. Wu and I. Shaknov, *Phys. Rev.* **77**, 136 (1950).
- [2] S. J. Freedman and J. F. Clauser, *Phys. Rev. Lett.* **28**, 938 (1972).
- [3] L. R. Kasday, J. D. Ullman, and C.-S. Wu, *Il Nuovo Cimento B* (1971-1996) **25**, 633 (1975).
- [4] A. Aspect, J. Dalibard, and G. Roger, *Phys. Rev. Lett.* **49**, 1804 (1982).
- [5] G. Weihs, T. Jennewein, C. Simon, H. Weinfurter, and A. Zeilinger, *Physical Review Letters* **81**, 5039–5043 (1998).
- [6] Y. Afik and J. R. M. n. de Nova, *Eur. Phys. J. Plus* **136**, 907 (2021), arXiv:2003.02280 [quant-ph].
- [7] M. Fabbrichesi, R. Floreanini, and G. Panizzo, *Phys. Rev. Lett.* **127**, 161801 (2021), arXiv:2102.11883 [hep-ph].
- [8] C. Severi, C. D. E. Boschi, F. Maltoni, and M. Sioli, *Eur. Phys. J. C* **82**, 285 (2022), arXiv:2110.10112 [hep-ph].
- [9] Y. Afik and J. R. M. n. de Nova, *Quantum* **6**, 820 (2022), arXiv:2203.05582 [quant-ph].
- [10] Y. Afik and J. R. M. de Nova, *Phys. Rev. Lett.* **130**, 221801 (2023), arXiv:2209.03969 [quant-ph].
- [11] T. Han, M. Low, and T. A. Wu, *JHEP* **07**, 192 (2024), arXiv:2310.17696 [hep-ph].
- [12] J. A. Aguilar-Saavedra and J. A. Casas, *Eur. Phys. J. C* **82**, 666 (2022), arXiv:2205.00542 [hep-ph].
- [13] Z. Dong, D. Gonçalves, K. Kong, and A. Navarro, *Phys. Rev. D* **109**, 115023 (2024), arXiv:2305.07075 [hep-ph].
- [14] K. Cheng, T. Han, and M. Low, *Phys. Rev. D* **109**, 116005 (2024), arXiv:2311.09166 [hep-ph].
- [15] K. Cheng, T. Han, and M. Low, *Phys. Rev. D* **111**, 033004 (2025), arXiv:2407.01672 [hep-ph].
- [16] T. Han, M. Low, N. McGinnis, and S. Su, *JHEP* **05**, 081 (2025), arXiv:2412.21158 [hep-ph].
- [17] Y. Afik, R. Demina, A. Herrera, O. Heinz Hindrichs, J. R. M. de Nova, and B. Ravina, (2026), arXiv:2602.15115 [quant-ph].
- [18] M. M. Altakach, P. Lamba, F. Maltoni, K. Mawatari, and K. Sakurai, *Phys. Rev. D* **107**, 093002 (2023), arXiv:2211.10513 [hep-ph].
- [19] K. Ehatäht, M. Fabbrichesi, L. Marzola, and C. Veelken, *Phys. Rev. D* **109**, 032005 (2024), arXiv:2311.17555 [hep-ph].
- [20] K. Ma and T. Li, *Chin. Phys. C* **48**, 103105 (2024), arXiv:2309.08103 [hep-ph].
- [21] M. Fabbrichesi and L. Marzola, *Phys. Rev. D* **110**, 076004 (2024), arXiv:2405.09201 [hep-ph].
- [22] T. Han, M. Low, and Y. Su, (2025), arXiv:2501.04801 [hep-ph].
- [23] R. A. Morales, *Eur. Phys. J. C* **84**, 581 (2024), arXiv:2403.18023 [hep-ph].
- [24] Y. Zhang, B.-H. Zhou, Q.-B. Liu, S. Li, S.-C. Hsu, T. Han, M. Low, and T. A. Wu, (2025), arXiv:2504.01496 [hep-ph].
- [25] T. Ai, Q. Bi, Y. He, J. Liu, and X.-P. Wang, *Phys. Rev. Lett.* **135**, 241804 (2025), arXiv:2506.10673 [hep-ph].
- [26] A. J. Barr, *Phys. Lett. B* **825**, 136866 (2022), arXiv:2106.01377 [hep-ph].
- [27] A. J. Barr, P. Caban, and J. Rembieliński, *Quantum* **7**, 1070 (2023), arXiv:2204.11063 [quant-ph].
- [28] R. Ashby-Pickering, A. J. Barr, and A. Wierzychucka, *JHEP* **05**, 020 (2023), arXiv:2209.13990 [quant-ph].
- [29] J. A. Aguilar-Saavedra, A. Bernal, J. A. Casas, and J. M. Moreno, *Phys. Rev. D* **107**, 016012 (2023), arXiv:2209.13441 [hep-ph].
- [30] M. Fabbrichesi, R. Floreanini, E. Gabrielli, and L. Marzola, *Eur. Phys. J. C* **83**, 823 (2023), arXiv:2302.00683 [hep-ph].
- [31] F. Fabbri, J. Howarth, and T. Maurin, *Eur. Phys. J. C* **84**, 20 (2024), arXiv:2307.13783 [hep-ph].
- [32] Q. Bi, Q.-H. Cao, K. Cheng, and H. Zhang, *Phys. Rev. D* **109**, 036022 (2024), arXiv:2307.14895 [hep-ph].
- [33] R. A. Morales, *Eur. Phys. J. Plus* **138**, 1157 (2023), arXiv:2306.17247 [hep-ph].
- [34] A. Bernal, P. Caban, and J. Rembieliński, *Sci. Rep.* **15**, 23410 (2025), arXiv:2405.16525 [hep-ph].
- [35] M. Grossi, G. Pelliccioli, and A. Vicini, *JHEP* **12**, 120 (2024), arXiv:2409.16731 [hep-ph].
- [36] D. Gonçalves, A. Kaladharan, F. Krauss, and A. Navarro, (2025), arXiv:2505.12125 [hep-ph].
- [37] D. Gonçalves, A. Kaladharan, and A. Navarro, (2025), arXiv:2506.19951 [hep-ph].
- [38] J. A. Aguilar-Saavedra, *Phys. Rev. D* **107**, 076016 (2023), arXiv:2209.14033 [hep-ph].
- [39] J. A. Aguilar-Saavedra, *Eur. Phys. J. C* **85**, 969 (2025), arXiv:2505.11870 [hep-ph].
- [40] R. Ding, A. Ruzi, S. Qian, A. Levin, Y. Wu, and Q. Li, (2025), arXiv:2504.09832 [hep-ph].
- [41] G. Aad *et al.* (ATLAS), (2026), arXiv:2603.26463 [hep-ex].
- [42] (2025).
- [43] Y. Du, X.-G. He, C.-W. Liu, and J.-P. Ma, (2024), arXiv:2409.15418 [hep-ph].
- [44] Y. Afik, Y. Kats, J. R. M. de Nova, A. Soffer, and D. Uzan, *Phys. Rev. D* **111**, L111902 (2025), arXiv:2406.04402 [hep-ph].
- [45] S. Chen, Y. Nakaguchi, and S. Komamiya, *PTEP* **2013**, 063A01 (2013), arXiv:1302.6438 [hep-ph].
- [46] J. Pei, X. Hao, X. Wang, and T. Li, (2025), arXiv:2505.09931 [hep-ph].
- [47] J. Pei, T. Li, L. Wu, X. Hao, and X. Wang, (2025), arXiv:2510.08031 [hep-ph].
- [48] M. Fucilla and Y. Hatta, *Phys. Rev. D* **113**, L031504 (2026), arXiv:2509.05267 [hep-ph].
- [49] K. Cheng and B. Yan, *Phys. Rev. Lett.* **135**, 011902 (2025), arXiv:2501.03321 [hep-ph].
- [50] S.-J. Lin, M.-J. Liu, D. Y. Shao, and S.-Y. Wei, (2025), arXiv:2507.15387 [hep-ph].
- [51] K. Cheng, T. Han, M. Low, and T. A. Wu, (2025), arXiv:2507.12513 [hep-ph].
- [52] Y.-C. Guo, T. Han, M. Low, and Y. Su, (2026), arXiv:2602.02719 [hep-ph].
- [53] Y.-J. Fang, A. Bhoonah, K. Cheng, T. Han, Y. Liu, and

- H. Zhang, (2026), arXiv:2604.11887 [hep-ph].
- [54] W. Qi, Z. Guo, and B.-W. Xiao, Phys. Rev. D **113**, 054048 (2026), arXiv:2506.12889 [hep-ph].
- [55] K. Cheng, T. Han, and S. Trifinopoulos, (2025), arXiv:2510.23773 [hep-ph].
- [56] Y. Hatta and J. Schoenleber, Phys. Rev. D **113**, 094016 (2026), arXiv:2511.04537 [hep-ph].
- [57] A. Ruzi, Y. Wu, R. Ding, and Q. Li, Chin. Phys. C **50**, 023103 (2026), arXiv:2506.16077 [hep-ph].
- [58] Q.-H. Cao, G. Li, X.-K. Wen, and B. Yan, (2025), arXiv:2509.18276 [hep-ph].
- [59] H.-L. Feng, H. Tang, W.-z. Guo, and Q. Qin, Phys. Rev. D **112**, 036020 (2025), arXiv:2504.15798 [hep-ph].
- [60] M. Fucilla, Y. Hatta, and B.-W. Xiao, (2026), arXiv:2604.11697 [hep-ph].
- [61] H.-W. Zhang, X. Cao, and T.-F. Feng, (2026), arXiv:2602.10389 [hep-ph].
- [62] Y.-X. Liu, W. Qi, L.-T. He, and B.-W. Xiao, (2026), arXiv:2604.17756 [hep-ph].
- [63] D. Wang, X. Hao, L. Liu, L. Wu, and T. Li, (2026), arXiv:2605.13250 [hep-ph].
- [64] D. Gonçalves, A. Kaladharan, and A. Navarro, (2026), arXiv:2604.16218 [hep-ph].
- [65] Y. Du, C.-Q. Geng, X.-G. He, C.-W. Liu, S.-L. Liu, and X.-Y. Liu, (2026), arXiv:2605.09682 [hep-ph].
- [66] B. Yang, Y. Zhang, Z. S. Wang, and X. Zhou, (2026), arXiv:2603.05846 [hep-ph].
- [67] C. Li, X. Cao, A.-Q. Guo, C.-X. Yu, H.-W. Zhang, and Z. Zhang, (2026), arXiv:2602.10398 [hep-ph].
- [68] J. Pei, L. Wu, D. Wang, X. Hao, and T. Li, (2026), arXiv:2601.15748 [hep-ph].
- [69] J. Pei, L. Wu, T. Li, and X. Hao, (2026), arXiv:2601.15747 [hep-ph].
- [70] G. Aad *et al.* (ATLAS), Nature **633**, 542 (2024), arXiv:2311.07288 [hep-ex].
- [71] A. Hayrapetyan *et al.* (CMS), Rept. Prog. Phys. **87**, 117801 (2024), arXiv:2406.03976 [hep-ex].
- [72] J. S. Bell, Physics Physique Fizika **1**, 195 (1964).
- [73] S. A. Abel, M. Dittmar, and H. K. Dreiner, Phys. Lett. B **280**, 304 (1992).
- [74] S. Li, W. Shen, and J. M. Yang, Eur. Phys. J. C **84**, 1195 (2024), arXiv:2401.01162 [hep-th].
- [75] P. Bechtle, C. Breuning, H. K. Dreiner, and C. Duhr, (2025), arXiv:2507.15947 [hep-ph].
- [76] S. A. Abel, H. K. Dreiner, R. Sengupta, and L. Ubaldi, (2025), arXiv:2507.15949 [hep-ph].
- [77] M. Low, Phys. Rev. D **112**, 096008 (2025), arXiv:2508.10979 [hep-ph].
- [78] J. A. Aguilar-Saavedra, J. A. Casas, and J. M. Moreno, (2026), arXiv:2603.19389 [hep-ph].
- [79] Y. Afik *et al.*, Eur. Phys. J. Plus **140**, 855 (2025), arXiv:2504.00086 [hep-ph].
- [80] K. Cheng, T. Han, and M. Low, Phys. Lett. B **868**, 139675 (2025), arXiv:2410.08303 [hep-ph].
- [81] G. Hanson *et al.*, Phys. Rev. Lett. **35**, 1609 (1975).
- [82] J. R. Ellis and I. Karliner, Nucl. Phys. B **148**, 141 (1979).
- [83] R. Brandelik *et al.* (TASSO), Phys. Lett. B **97**, 453 (1980).
- [84] R. Plano, A. Prodell, N. Samios, M. Schwartz, and J. Steinberger, Phys. Rev. Lett. **3**, 525 (1959).
- [85] N. P. Samios, R. Plano, A. Prodell, M. Schwartz, and J. Steinberger, Phys. Rev. **126**, 1844 (1962).
- [86] A. Abashian *et al.* (Belle), Nucl. Instrum. Meth. A **479**, 117 (2002).
- [87] J. F. Clauser, M. A. Horne, A. Shimony, and R. A. Holt, Phys. Rev. Lett. **23**, 880 (1969).
- [88] T. Abe *et al.* (Belle-II), (2010), arXiv:1011.0352 [physics.ins-det].
- [89] W. K. Wootters, Phys. Rev. Lett. **80**, 2245 (1998), arXiv:quant-ph/9709029.
- [90] F. Verstraete and M. M. Wolf, Phys. Rev. Lett. **89**, 170401 (2002), arXiv:quant-ph/0112012.
- [91] J. Alwall, M. Herquet, F. Maltoni, O. Mattelaer, and T. Stelzer, JHEP **06**, 128 (2011), arXiv:1106.0522 [hep-ph].
- [92] B. Aubert *et al.* (BaBar), Nucl. Instrum. Meth. A **479**, 1 (2002), arXiv:hep-ex/0105044.
- [93] J. Brodzicka *et al.* (Belle), PTEP **2012**, 04D001 (2012), arXiv:1212.5342 [hep-ex].
- [94] BESIII Collaboration, “BESIII data taking at the  $\psi(3770)$  energy region,” (2024), [https://english.ihep.cas.cn/nw/han/y24/202403/t20240305\\_657949.html](https://english.ihep.cas.cn/nw/han/y24/202403/t20240305_657949.html).
- [95] H. Ollivier and W. H. Zurek, Phys. Rev. Lett. **88**, 017901 (2001), arXiv:quant-ph/0105072.
- [96] S. Luo, Phys. Rev. A **77**, 042303 (2008).
- [97] S. Wu, C. Qian, Q. Wang, and Y.-G. Yang, Phys. Rev. D **113**, 056030 (2026), arXiv:2509.14990 [hep-ph].
- [98] H.-W. Zhang, X. Cao, and T.-F. Feng, (2026), arXiv:2605.19642 [hep-ph].
- [99] C. D. White and M. J. White, Phys. Rev. D **110**, 116016 (2024), arXiv:2406.07321 [hep-ph].
- [100] J. Gargalionis, N. Moynihan, S. Trifinopoulos, E. N. V. Wallace, C. D. White, and M. J. White, Phys. Rev. D **113**, 016007 (2026), arXiv:2508.14967 [hep-th].
- [101] CMS collaboration, (2025), CMS-PAS-TOP-25-001.